

**Occurrence of new phosphides and sulfide of Ni, Co, V, and Mo from chromitite of the Othrys ophiolite complex (Central Greece)**Federica Zaccarini ^{1,*}, Elena Ifandi ^{2,3}, Basilios Tsikouras ²,
Tassos Grammatikopolous ⁴, Giorgio Garuti ¹, Daniela Mauro ⁵, Luca Bindi ⁶,
Chris Stanley ⁷¹ Department of Applied Geological Sciences and Geophysics, University of Leoben, A-8700 Leoben, Austria² Faculty of Science, Physical and Geological Sciences, Universiti Brunei Darussalam, BE 1410 Gadong, Brunei Darussalam³ Department of Geology, Section of Earth Materials, University of Patras, 265 00 Patras, Greece⁴ SGS Canada Inc., 185 Concession Street, PO 4300, Lakefield, Ontario K0L 2H0, Canada⁵ Department of Earth Sciences, University of Pisa, I-56126 Pisa, Italy⁶ Department of Earth Sciences, University of Firenze, I-50121 Firenze, Italy⁷ Department of Earth Sciences, Natural History Museum, London SW7 5BD, UK**ARTICLE INFO**

Submitted: February 2019

Accepted: April 2019

Available on line: xxxxxx 2019

* Corresponding author:
federica.zaccarini@unileoben.ac.at

DOI: 10.2451/2019PM851

How to cite this article:
Zaccarini F. et al. (2019)
Period. Mineral. 88, xx-xx**ABSTRACT**

Unnamed phosphides of Ni, Co, V, Mo, and one V-sulfide were found in a chromitite of the Agios Stefanos mine (Othrys ophiolite, Central Greece). Most of the phosphides have a stoichiometry similar to allabogdanite or barringerite but show significant proportions of Co, V, and Mo. The minerals could correspond to a Ni-allabogdanite or Ni-barringerite, and to a V-allabogdanite or V-barringerite. More complex stoichiometries are observed when Mo is the dominant metal, and thus it leads to a potentially new $(\text{Mo}, \text{V}, \text{Fe})_3(\text{Ni}, \text{Co})_2\text{P}$ mineral. The sulfide corresponds to the ideal formula VS. All the grains vary in size between 5 and 80 μm , and show distinctive reflectance and optical properties. In contrast, Raman spectra are not significantly distinctive. The rare minerals occur intergrown with brecciated chromite, awaruite, and various sulfides produced by alteration of chromitite under reducing conditions. Interpretation of their origin is still speculative embracing a number of possible processes: i) high-temperature reaction of the chromitites with reducing fluids, at mantle depth, ii) low-temperature alteration during serpentinization, iii) post-orogenic, surface lightning strike, or iv) meteorite impact. The minerals described in this work potentially represent new mineral species that are still under study for a complete crystallographic characterization, as required for the acceptance by the IMA Commission on New Minerals, Nomenclature and Classification.

Keywords: new minerals; Ni-V-Co-phosphides; V-sulfide; chromitite; Agios Stefanos mine; ophiolite; Othrys; Greece.

INTRODUCTION

According to the IMA list dated March 2019 (<http://cnmnc.main.jp/>), 5467 minerals have been accepted as valid species. The V-bearing minerals are rare, representing only less than the 5% of the approved

minerals and only 8 of them are sulfides and sulfosalts. They include colimaite, K_3VS_4 (Ostrooumov et al., 2009), colusite, $\text{Cu}_{26}\text{V}_2(\text{As}, \text{Sn}, \text{Sb})_6\text{S}_{32}$ (Zachariassen, 1933), germanocolusite $\text{Cu}_{26}\text{V}_2(\text{Ge}, \text{Sn}, \text{Sb})_6\text{S}_{32}$ (Spiridov et al., 1992a), merelaniite $(\text{Mo}_4\text{Pb}_4\text{VSbS}_{15})$ (Jaszczak et al.,

2016), nekrasovite, $\text{Cu}_{26}\text{V}_2(\text{Sn,As,Sb})_6\text{S}_{32}$ (Kovalenker et al., 1984), patronite, VS_4 (Hewett, 1910), stibicolusite, $\text{Cu}_{26}\text{V}_2(\text{Sb,Sn,As})_6\text{S}_{32}$ (Spiridonov et al., 1992b) and sulvanite, Cu_3VS_4 (Trojer, 1966). Most of the V-sulfides and sulfosalts, with the exception of patronite, a mineral discovered in 1906 in the Mina Ragra of Peru (Hewett, 1910), are characterized by a complex composition. Phosphides are also rare in nature and only 14 phases (see IMA list dated March 2019) are officially accepted, including: allabogdanite $(\text{Fe,Ni})_2\text{P}$ (Britvin et al., 2002), andreyivanovite $\text{Fe}(\text{Cr,Fe})\text{P}$ (Zolensky et al., 2008), barringerite $(\text{Fe,Ni})_2\text{P}$ (Buseck, 1969), florenskyite $\text{Fe}(\text{Ti,Ni})\text{P}$ (Ivanov et al., 2000), halamishite Ni_5P_4 (Britvin et al., 2014), melliniite $(\text{Ni,Fe})_4\text{P}$ (Pratesi et al., 2006), monipite MoNiP (Ma et al., 2014), murashkoite FeP (Britvin et al., 2013, 2019), negevite NiP_2 (Britvin et al., 2014), nickelporphide $(\text{Ni,Fe})_3\text{P}$ (Britvin et al., 1999), nickolayite FeMoP (Murashko et al., 2019), schreibersite $(\text{Fe,Ni})_3\text{P}$ (Skala and Cisarova, 2005 and references therein), transjordanite Ni_2P (Britvin et al., 2014) and zuktamurrite FeP_2 (Britvin et al., 2014, 2018). Recently, Zaccarini et al. (2016), Ifandi et al. (2018) and Sideridis et al. (2018) have described the mineral chemistry of several potentially new phosphides found in chromitites of the ophiolites of Othrys and Gerakini-Ormylia (Greece) and Alapaevsk (Russia). The phosphides from the Gerakini-Ormylia and Alapaevsk exhibit a stoichiometry close to $(\text{Ni,Fe})_5\text{P}$, and those from Othrys can be classified either as Ni-allabogdanite or Ni-barringerite and V-allabogdanite or V-barringerite. All the grains described by Zaccarini et al. (2016), Ifandi et al. (2018) and Sideridis et al. (2018) were too small ($<20 \mu\text{m}$) to be investigated by X-ray diffraction. Therefore, the only data available on these rare phosphides are limited to electron microprobe analyses and description of their morphology and colour.

In this paper, we report for the first time a more detailed mineralogical characterization based on a new set of electron microprobe analyses, Raman spectroscopy and reflectance values obtained on accessory minerals found in a new sample of the Othrys chromitite. The new data show that the Othrys chromitite represents a source of extremely rare and potentially new phosphides in the system V-Ni-Mo and a V-sulfide.

SAMPLE DESCRIPTION AND METHODOLOGY

The V-Ni-Mo phosphides and the V-sulfide described in the present work were observed in new heavy-mineral concentrates obtained from the same chromitite sample studied by Ifandi et al. (2018), collected in the Agios Stefanos abandoned mine of the Othrys ophiolite (Figure 1 A,B). The studied sample consists of massive chromitite, hosted in a strongly serpentinized dunite body within a mantle tectonite composed of harzburgite

and less plagioclase-lherzolite (Economou et al., 1986; Garuti et al., 1999; Tsikouras et al., 2016). Mafic rocks, mainly gabbros of the crustal sequence and gabbro dykes, have been also recognized (Figure 1C). The chromitite from the sample locality has a massive texture, but locally shows breccia-type deformation visible under the microscope (Figure 2 A,B). The spinel has heterogeneous composition corresponding to magnesiochromite (Ifandi et al., 2018) with Cr_2O_3 (44.96-51.64 wt%), Al_2O_3 (14.18-20.78 wt%), MgO (13.34-16.84 wt%), and FeO (8.3-13.31 wt%). Calculated Fe_2O_3 ranges from 6.72 to 9.26 wt%. The amounts of minor elements MnO (0.33-0.60 wt%), V_2O_3 (0.04-0.3 wt%), ZnO (up to 0.07 wt%) and NiO (0.03-0.24 wt%) exhibit minor variations. MnO (0.33-0.60 wt%), V_2O_3 (0.04-0.3 wt%), ZnO (up to 0.07 wt%) and NiO (0.03-0.24 wt%). The TiO_2 content is low

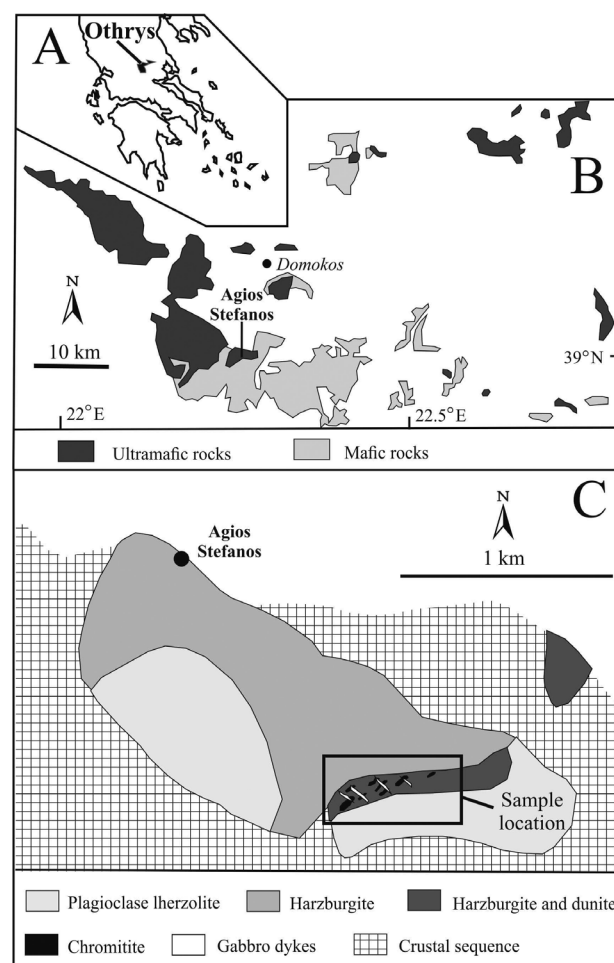


Figure 1. Location of the Othrys complex in Greece (A), general geological map of the Othrys ophiolite showing location of the Agios Stefanos chromium mine (B) and (C) detailed geology of the Agios Stefanos area. (Modified after Rassios and Smith, 2001; Ifandi et al., 2018).

(0.03-0.23 wt%) consistent with most mantle-hosted podiform chromitites. The Cr/(Cr+Al) ratios are lower than those typical of chromites with a boninitic affinity (Ifandi et al., 2018).

The processing and recovery of the heavy minerals was carried out treating about 10 kg of massive chromitite at SGS Mineral Services, Canada, following the procedure described by Ifandi et al. (2018). The heavy minerals were prepared in epoxy blocks, and then polished for the mineralogical examination. The polished blocks were previously studied in the Laboratory of Mineralogy Petrology and Geochemistry, Faculty of Science, Universiti Brunei Darussalam using a Scanning Electron Microscope (SEM) equipped with energy dispersive spectrometer (EDS) with an accelerating voltage of 20 kV and a beam current of 6 nA. Subsequently, they were carefully investigated with a reflected-light microscope at 250-800X magnification, at the University of Leoben, Austria. The V-Ni-Mo minerals, larger than 10 microns, were quantitatively analyzed with a Superprobe Jeol JXA 8200 at the University of Leoben, Austria in the WDS mode. Analytical conditions were 20 kV accelerating voltage, 10 nA beam current, and beam diameter of about 1 micron. The peak and background counting times were 20 and 10s, respectively. The $K\alpha$ lines were used for all the elements, with the exception of $L\alpha$ that were selected for Ir and Mo. The reference materials were chromite, skutterudite, metallic vanadium, molybdenite, and synthetic Ni_3P and Fe_3P . The following diffracting crystals were selected: PETJ for P and Mo, and LIFH for Fe, Co, Ni, Cr and V. In most of the analyzed grains, Cr was found below the detection limit of the instrument. The results are presented in Table 1. The same conditions were used to obtain the X-ray elemental distribution maps.

Reflectance measurements were made in air relative to a $WTiC$ standard on selected V- and Ni-phases using a J and M TIDAS diode array spectrometer attached to a Zeiss Axiotron microscope, at the Natural History Museum of London, UK. Measurements were made on unoriented grains at extinction positions leading to the designation of R_1 (minimum) and R_2 (maximum) (Table 2).

Unpolarized micro-Raman spectra were collected at the University of Pisa, Italy, using a Jobin-Yvon Horiba XploRA Plus apparatus equipped with a motorized x-y-stage and an Olympus BX41 microscope with a 100 \times objective. The 532 nm line of a solid-state laser was used. The minimum lateral and depth resolution was set to a few μm . The system was calibrated using the 520.6 cm^{-1} Raman band of silicon before each experimental session. Spectra were collected through multiple acquisitions with single counting times of 120 s, with the laser power filtered at 1%. The backscattered radiation was analyzed with a 1200 mm^{-1} grating monochromator. However, the preliminary

results suggest that the micro-Raman spectroscopy is not appropriate to study the potential new minerals reported in this contribution, as their spectra are very similar despite of the difference in their chemical composition.

RESULTS

Textural relations of the potential new minerals

About 50 grains of V-Ni-Mo phosphides and V-sulfide were discovered in 1-inch polished block of chromite concentrate. The grains are usually less than 15 μm in size, but exceptionally may reach 80 μm , and can occur either as single phase grains or composite particles with other rare minerals such as Co-rich awaruite, pentlandite, native vanadium, melliniite, nickelphosphide, Mo-Ni-V-Co alloy (probably hexamolybdenum), Hg-selenide (possibly tiemannite), chromite, chlorite, quartz and glass (Ifandi et al., 2018). One large composite particle illustrates the textural relations between chromite and the phosphide-bearing ore assemblage (Figure 2 C,D). The X-ray elemental distribution maps show that the grain mainly consists of a likely Ni-Co awaruite (Figure 2 E,F) containing small blebs of (Fe,Ni)- and Ni-phosphide (Figure 2 G,H), and pentlandite (Figure 2I). The metallic phases are intimately intergrown with chromite displaying the same composition and breccia-type texture as the in situ chromitite (Figure 2D). Selected back-scattered electron (BSE) and reflected-light microscope images of the phosphides and the V-sulfide assemblages are illustrated in Figures 3 and 4. Textural details indicate that phosphides with different compositions (melliniite, nickelphosphide, and the new V-Ni-Mo phosphides) occur mainly associated with awaruite (Figures 3 E,G and 4 A,C,E,G), possibly representing secondary phases. The same is concluded for the unnamed V-sulfide (Figures 4 C,E,G). The single-phase grains (Figures 3 A,C) may indicate a complete replacement of previous awaruite, or direct precipitation from a P-rich metasomatic fluid.

Mineral chemistry and optical properties

The unnamed minerals recovered from the Othrys chromitite are phosphides with variable stoichiometry from M_2P (10 grains) to M_3P (one grain), and one unnamed vanadium sulfide. Electron microprobe analyses of these minerals are presented in Table 1 as elemental concentrations expressed in wt%, at%, and recalculated number of atoms per formula unit (apfu). Optical properties have been measured for the largest grains. Values of the reflectance are listed in Table 2, and graphically illustrated in Figure 5.

Ni-allabogdanite or Ni-barringerite and V-allabogdanite or V-barringerite

Electron microprobe analyses indicate that the phosphides with M_2P stoichiometry are compositionally

Table 1. Electron microprobe analyses of the potential new minerals in the Othrsy chromitite.

Sample	wt%								
	P	S	V	Cr	Fe	Co	Ni	Mo	Total
Phosphides									
Ni-allabogdanite or Ni-barringerite									
Grain 14									
ot2gr14an2	19.22	0.59	4.40	0.00	6.62	17.84	20.16	31.30	100.13
ot2gr14an1	19.67	0.62	4.80	0.00	5.18	18.03	20.48	32.00	100.78
Grain 15									
ot2gr15an2	21.04	0.36	18.57	0.00	3.07	18.24	22.72	17.62	101.63
ot2gr15an1	20.96	0.33	19.01	0.00	3.12	19.04	23.14	15.39	100.98
Grain 13									
ot2gr13an2	21.47	0.34	20.30	0.00	3.14	17.99	23.87	13.66	100.77
ot2gr13an4	21.63	0.33	20.33	0.00	3.17	17.67	23.63	13.83	100.59
ot2gr13an3	21.38	0.35	20.28	0.00	3.20	17.76	23.69	13.66	100.32
ot2gr13an1	21.31	0.33	20.57	0.00	3.16	17.74	23.83	13.55	100.49
Grain 21									
ot2gr21an1	21.63	0.28	20.89	0.00	2.99	18.25	24.43	13.08	101.55
V-allabogdanite or V-barringerite									
Grain 7									
ot2gr7an2	21.27	0.28	20.72	0.00	3.52	18.49	23.10	12.93	100.31
ot2gr7an3	21.07	0.32	20.80	0.00	3.54	15.83	23.13	16.03	100.72
Grain 21									
ot2gr21an2	21.18	0.27	21.04	0.00	3.04	18.14	24.11	13.10	100.88
Grain 22									
ot2gr22an11	21.40	0.26	21.17	0.00	2.83	18.23	24.29	12.23	100.40
Grain 5									
ot2gr5an3	21.23	0.32	21.14	0.00	3.07	15.08	24.22	15.76	100.81
ot2gr5an1	21.38	0.29	21.21	0.00	3.13	16.94	23.40	13.68	100.02
Grain 3									
ot2gr3an3	21.66	0.29	21.37	0.00	3.17	18.11	23.40	12.34	100.34
Grain 25									
ot2gr25an2	21.28	0.26	24.19	0.00	2.93	14.42	23.94	13.52	100.54
ot2gr25an1	21.19	0.24	24.55	0.00	2.90	14.66	23.57	13.37	100.47
(Mo,Ni,V) ₅ P									
Grain 17									
ot2gr17an4	7.59	0.64	14.19	0.00	1.14	7.47	23.78	43.56	98.37
ot2gr17an3	7.96	0.67	14.18	0.00	1.18	7.72	23.77	44.04	99.53
ot2gr17an5	8.03	0.65	14.16	0.00	1.18	7.53	24.16	44.16	99.87
ot2gr17an2	8.05	0.71	13.98	0.00	1.19	7.56	23.86	44.39	99.73
ot2gr17an1	8.20	0.66	14.13	0.00	1.20	7.67	23.91	44.65	100.42
Sulfide									
VS									
Grain 22									
ot2gr22an1	0.08	38.06	57.76	0.00	0.67	0.52	1.86	0.86	99.81

Table 1.Continued...

wt%									
Sample	P	S	V	Cr	Fe	Co	Ni	Mo	Total
Phosphides									
Ni-allabogdanite or Ni-barringerite									
ot2gr22an2	0.02	38.18	57.81	0.00	0.70	0.48	1.68	0.81	99.68
ot2gr22an3	0.03	38.20	57.56	0.00	0.78	0.55	1.88	0.80	99.79
Grain 7									
ot2gr7an5	0.02	38.01	57.07	0.00	0.88	0.50	1.46	0.76	98.68
ot2gr7an4	0.00	38.17	57.22	0.00	0.91	0.54	1.38	0.82	99.02
Grain 6									
ot2gr6an1	0.03	38.27	57.75	0.00	0.83	0.63	1.87	0.80	100.18
ot2gr6an2	0.03	38.42	57.90	0.00	0.73	0.62	2.00	0.82	100.52
at%									
Sample	P	S	V	Cr	Fe	Co	Ni	Mo	Total
Phosphides									
Ni-allabogdanite or Ni-barringerite									
Grain 14									
ot2gr14an2	34.16	1.01	4.76	0.00	6.53	16.67	18.91	17.96	100
ot2gr14an1	34.72	1.05	5.15	0.00	5.07	16.72	19.07	18.23	100
Grain 15									
ot2gr15an2	34.13	0.57	18.31	0.00	2.77	15.55	19.45	9.23	100
ot2gr15an1	33.94	0.51	18.72	0.00	2.81	16.20	19.77	8.05	100
Grain 13									
ot2gr13an2	34.44	0.53	19.79	0.00	2.79	15.17	20.21	7.08	100
ot2gr13an4	34.73	0.51	19.84	0.00	2.83	14.91	20.02	7.17	100
ot2gr13an3	34.45	0.54	19.86	0.00	2.86	15.04	20.14	7.11	100
ot2gr13an1	34.28	0.52	20.12	0.00	2.82	15.00	20.23	7.04	100
Grain 21									
ot2gr21an1	34.35	0.43	20.17	0.00	2.63	15.23	20.47	6.71	100
V-allabogdanite or V-barringerite									
Grain 7									
ot2gr7an2	34.21	0.43	20.26	0.00	3.14	15.63	19.61	6.71	100
ot2gr7an3	34.15	0.50	20.50	0.00	3.18	13.49	19.79	8.39	100
Grain 21									
ot2gr21an2	33.94	0.42	20.50	0.00	2.70	15.28	20.39	6.78	100
Grain 22									
ot2gr22an11	34.28	0.40	20.61	0.00	2.52	15.34	20.53	6.32	100
Grain 5									
ot2gr5an1	34.51	0.45	20.81	0.00	2.80	14.37	19.93	7.13	100
ot2gr5an3	34.31	0.49	20.77	0.00	2.75	12.80	20.66	8.22	100
Grain 3									
ot2gr3an3	34.63	0.45	20.77	0.00	2.81	15.22	19.75	6.37	100
Grain 25									
ot2gr25an2	34.09	0.40	23.55	0.00	2.60	12.14	20.23	6.99	100

Table 1.Continued...

at%									
Sample	P	S	V	Cr	Fe	Co	Ni	Mo	Total
Phosphides									
Ni-allabogdanite or Ni-barringerite									
ot2gr25an1	33.95	0.37	23.91	0.00	2.58	12.34	19.92	6.92	100
(Mo,Ni,V) ₅ P									
Grain 17									
ot2gr17an4	15.81	1.29	17.97	0.00	1.32	8.18	26.14	29.29	100
ot2gr17an3	16.34	1.33	17.70	0.00	1.34	8.33	25.76	29.19	100
ot2gr17an5	16.42	1.29	17.61	0.00	1.34	8.10	26.08	29.16	100
ot2gr17an2	16.50	1.40	17.42	0.00	1.35	8.15	25.81	29.37	100
ot2gr17an1	16.69	1.30	17.47	0.00	1.36	8.20	25.67	29.32	100
Sulfide									
VS									
Grain 22									
ot2gr22an1	0.11	49.77	47.54	0.00	0.50	0.37	1.33	0.38	100
ot2gr22an2	0.03	49.95	47.60	0.00	0.53	0.34	1.20	0.35	100
ot2gr22an3	0.04	49.94	47.36	0.00	0.58	0.39	1.34	0.35	100
Grain 7									
ot2gr7an5	0.02	50.16	47.41	0.00	0.66	0.36	1.05	0.33	100
ot2gr7an4	0.00	50.20	47.38	0.00	0.69	0.38	0.99	0.36	100
Grain 6									
ot2gr6an1	0.04	49.85	47.36	0.00	0.62	0.45	1.33	0.35	100
ot2gr6an2	0.04	49.88	47.32	0.00	0.54	0.44	1.42	0.35	100
apfu									
Sample	P	S	V	Cr	Fe	Co	Ni	Mo	Total
Phosphides									
Ni-allabogdanite or Ni-barringerite									
Grain 14									
ot2gr14an2	1.02	0.03	0.14	0.00	0.20	0.50	0.57	0.54	3
ot2gr14an1	1.04	0.03	0.15	0.00	0.15	0.50	0.57	0.55	3
Grain 15									
ot2gr15an2	1.02	0.02	0.55	0.00	0.08	0.47	0.58	0.28	3
ot2gr15an1	1.02	0.02	0.56	0.00	0.08	0.49	0.59	0.24	3
Grain 13									
ot2gr13an2	1.03	0.02	0.59	0.00	0.08	0.45	0.61	0.21	3
ot2gr13an4	1.04	0.02	0.60	0.00	0.08	0.45	0.60	0.22	3
ot2gr13an3	1.03	0.02	0.60	0.00	0.09	0.45	0.60	0.21	3
ot2gr13an1	1.03	0.02	0.60	0.00	0.08	0.45	0.61	0.21	3
Grain 21									
ot2gr21an1	1.03	0.01	0.60	0.00	0.08	0.46	0.61	0.20	3
V-allabogdanite or V-barringerite									
Grain 7									
ot2gr7an2	1.03	0.01	0.61	0.00	0.09	0.47	0.59	0.20	3

Table 1.Continued...

Sample	apfu								
	P	S	V	Cr	Fe	Co	Ni	Mo	Total
Phosphides									
Ni-allabogdanite or Ni-barringerite									
ot2gr7an3	1.02	0.01	0.62	0.00	0.10	0.40	0.59	0.25	3
Grain 21									
ot2gr21an2	1.02	0.01	0.62	0.00	0.08	0.46	0.61	0.20	3
Grain 22									
ot2gr22an11	1.03	0.01	0.62	0.00	0.08	0.46	0.62	0.19	3
Grain 5									
ot2gr5an3	1.03	0.01	0.62	0.00	0.08	0.38	0.62	0.25	3
ot2gr5an1	1.04	0.01	0.62	0.00	0.08	0.43	0.60	0.21	3
Grain 3									
ot2gr3an3	1.04	0.01	0.62	0.00	0.08	0.46	0.59	0.19	3
Grain 25									
ot2gr25an2	1.02	0.01	0.71	0.00	0.08	0.36	0.61	0.21	3
ot2gr25an1	1.02	0.01	0.72	0.00	0.08	0.37	0.60	0.21	3
(Mo,Ni,V) ₅ P									
Grain 17									
ot2gr17an4	0.95	0.08	1.08	0.00	0.08	0.49	1.57	1.76	6
ot2gr17an3	0.98	0.08	1.06	0.00	0.08	0.50	1.55	1.75	6
ot2gr17an5	0.99	0.08	1.06	0.00	0.08	0.49	1.56	1.75	6
ot2gr17an2	0.99	0.08	1.05	0.00	0.08	0.49	1.55	1.76	6
ot2gr17an1	1.00	0.08	1.05	0.00	0.08	0.49	1.54	1.76	6
Sulfide									
VS									
Grain 22									
ot2gr22an1	0.00	1.00	0.95	0.00	0.01	0.01	0.03	0.01	2
ot2gr22an2	0.00	1.00	0.95	0.00	0.01	0.01	0.02	0.01	2
ot2gr22an3	0.00	1.00	0.95	0.00	0.01	0.01	0.03	0.01	2
Grain 7									
ot2gr7an5	0.00	1.00	0.95	0.00	0.01	0.01	0.02	0.01	2
ot2gr7an4	0.00	1.00	0.95	0.00	0.01	0.01	0.02	0.01	2
Grain 6									
ot2gr6an1	0.00	1.00	0.95	0.00	0.01	0.01	0.03	0.01	2
ot2gr6an2	0.00	1.00	0.95	0.00	0.01	0.01	0.03	0.01	2

similar to barringerite and allabogdanite, both having a composition of $(\text{Fe,Ni})_2\text{P}$, but orthorhombic and hexagonal symmetry, respectively. Barringerite was discovered in the Canyon Diablo nickel-iron meteorite, Coconino County, Arizona, USA (Buseck, 1969). Allabogdanite was found in the Onello meteorite, Bol'shoi Dolguchan River, Aldan shield, Sakha-Yakutia, Russia (Britvin et al., 2002). Both minerals are characterized by appreciable

amounts of Ni (up to more than 20 wt%), although Fe is always dominant over Ni. The new analyses from the Othrys phosphides confirm indicate that they are different from barringerite and allabogdanite because of their low Fe content, which is typically below 6.5 at%, the relatively high concentration of Ni, between 18.91 and 20.66 at%, and the significant substitution of Co, V, and Mo in the ranges of $\text{Co}=12.14\text{-}16.72$, $\text{V}=4.76\text{-}20.81$, and

Table 2. Reflectance data.

λ (nm)	NiP		VP				MoP				VS			
	Gr13	Gr13	Gr3	Gr3	Gr5	Gr5	Gr7	Gr7	Gr 17	Gr17	Gr6	Gr6	Gr7	Gr7
	R1	R2	R1	R2	R1	R2	R1	R2	R1	R2	R1	R2	R1	R2
400	47,8	48,1	47,7	48,2	48,5	48,7	47,6	48,8	54,4	54,6	32,0	33,1	32,3	32,4
420	48,5	48,8	48,0	48,5	48,7	48,9	47,9	49,1	54,7	54,9	32,7	33,7	33,0	33,0
440	49,3	49,6	48,4	48,9	49,0	49,2	48,3	49,4	55,0	55,2	33,5	34,5	33,7	33,7
460	50,1	50,4	48,8	49,5	49,5	49,7	48,6	49,9	55,3	55,5	34,3	35,3	34,5	34,5
480	50,9	51,2	49,3	50,0	50,1	50,4	49,0	50,7	55,6	55,8	35,2	36,1	35,3	35,4
500	51,7	52,1	49,8	50,7	50,9	51,1	49,4	51,5	55,9	56,1	36,1	37,0	36,2	36,3
520	52,6	53,0	50,3	51,4	51,7	51,9	49,9	52,4	56,1	56,4	36,9	37,8	37,1	37,2
540	53,5	53,9	50,9	52,2	52,4	52,6	50,3	53,3	56,4	56,7	37,7	38,7	38,0	38,1
560	54,3	54,7	51,4	52,9	53,3	53,5	50,9	54,1	56,7	57,0	38,6	39,7	39,0	39,0
580	55,1	55,5	51,9	53,5	54,0	54,2	51,4	54,9	57,0	57,3	39,5	40,8	39,9	39,9
600	55,7	56,1	52,5	54,1	54,7	54,9	51,9	55,5	57,4	57,6	40,5	41,9	40,7	40,9
620	56,4	56,7	53,0	54,7	55,6	55,8	52,4	56,2	57,8	58,0	41,2	42,9	41,4	41,7
640	56,9	57,2	53,4	55,2	56,3	56,5	53,0	56,8	58,1	58,3	42,1	43,8	42,2	42,5
660	57,3	57,6	53,7	55,6	57,0	57,2	53,4	57,4	58,4	58,6	42,8	44,6	42,8	43,2
680	57,6	57,9	54,2	56,0	57,7	57,9	53,8	58,0	58,7	58,9	43,5	45,5	43,5	43,9
700	58,1	58,4	54,9	56,6	58,4	58,6	54,2	58,6	58,9	59,2	44,3	46,2	44,3	44,6

NiP = Ni-allabogdanite or Ni-barringerite, VP = V-allabogdanite or Ni-barringerite, MoP = Mo-phosphide and VS = V-sulfide.

Mo=6.32-18.23 at% (Table 1). Based on the dominant metal, the minerals can be classified as Ni-allabogdanite or Ni-barringerite, and V-allabogdanite or V-barringerite, corresponding to the following stoichiometries:

Ni-allabogdanite or Ni-barringerite:

Grain 14, $(P_{1.03}S_{0.03})\Sigma_{1.06}(V_{0.15}Fe_{0.17}Co_{0.5}Ni_{0.57}Mo_{0.54})\Sigma_{1.94}$

Grain 15, $(P_{1.02}S_{0.02})\Sigma_{1.04}(V_{0.56}Fe_{0.08}Co_{0.48}Ni_{0.59}Mo_{0.26})\Sigma_{1.96}$

Grain 13, $(P_{1.03}S_{0.02})\Sigma_{1.05}(V_{0.6}Fe_{0.08}Co_{0.45}Ni_{0.6}Mo_{0.21})\Sigma_{1.95}$

Grain 21, $(P_{1.03}S_{0.01})\Sigma_{1.04}(V_{0.6}Fe_{0.08}Co_{0.46}Ni_{0.61}Mo_{0.2})\Sigma_{1.96}$

V-allabogdanite or V-barringerite

Grain 7, $(P_{1.02}S_{0.01})\Sigma_{1.03}(V_{0.62}Fe_{0.08}Co_{0.46}Ni_{0.62}Mo_{0.2})\Sigma_{1.97}$

Grain 21, $(P_{1.02}S_{0.01})\Sigma_{1.03}(V_{0.62}Fe_{0.08}Co_{0.46}Ni_{0.61}Mo_{0.2})\Sigma_{1.97}$

Grain 22, $(P_{1.03}S_{0.01})\Sigma_{1.04}(V_{0.62}Fe_{0.08}Co_{0.46}Ni_{0.62}Mo_{0.19})\Sigma_{1.96}$

Grain 5, $(P_{1.04}S_{0.01})\Sigma_{1.05}(V_{0.62}Fe_{0.08}Co_{0.41}Ni_{0.61}Mo_{0.23})\Sigma_{1.95}$

Grain 3, $(P_{1.04}S_{0.01})\Sigma_{1.05}(V_{0.62}Fe_{0.08}Co_{0.43}Ni_{0.59}Mo_{0.19})\Sigma_{1.95}$

Grain 25, $(P_{1.02}S_{0.01})\Sigma_{1.03}(V_{0.72}Fe_{0.08}Co_{0.36}Ni_{0.6}Mo_{0.21})\Sigma_{1.97}$

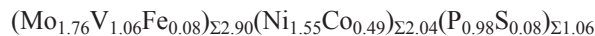
We have decided to assign the minor S to the P sites, but given the intermetallic character of most of the crystal structures of these phosphides S could be hosted in the metal sites as well.

The Ni-allabogdanite or Ni-barringerite and their vanadium varieties have comparable optical properties

in reflected-light (colour, reflectance, anisotropy). They appear creamy-yellowish, anisotropic (Figures 3 B,D,F,H, and 4 B,D,F,H), and exhibit similar variation of the reflectance (R_1 and R_2) (Figure 5 A,B; and Table 2).

Mo-phosphide, ideally $(Mo,V)_3(Ni,Co)_2P$

One single-phase grain, about 80 μm in size, was analysed in the Othrys chromitite (Figures 3C and D). Five spot analyses of the grain (Grain 17), yield the average composition (in wt%) of: P=7.97, S=0.67, V=14.13, Fe=1.18, Co=7.59, Ni=23.9, and Mo=44.16 (Table 1), corresponding to the empirical formula calculated on 6 atoms:



that can be approximated to ideal $(Mo,V,Fe)_3(Ni,Co)_2P$. This mineral was not previously described from the Othrys chromitites (Ifandi et al., 2018). Its composition is not consistent with either monipite (Ma et al., 2014) or nickolayite $FeMoP$ (Murashko et al., 2019). According to the metal:phosphorous ratio (5:1), the Othrys phosphide could represent the Mo equivalent of the grains recently found in chromitites of the Alapaevsk (Russia) and

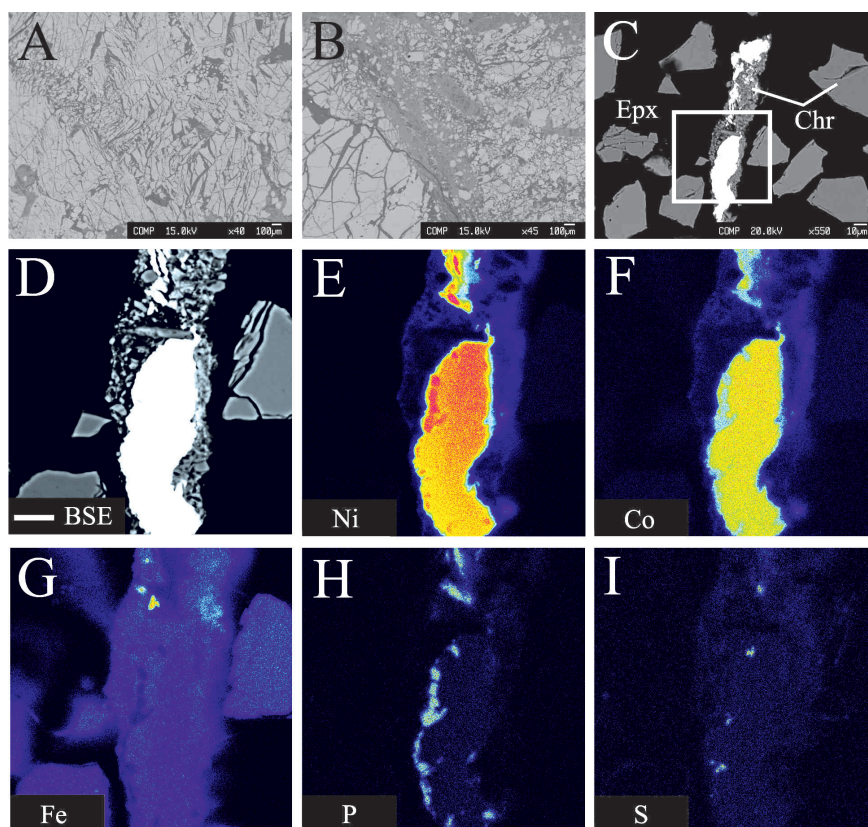


Figure 2. Back-scattered electron images (BSE) of brecciated chromitite from polished sections (A, B) and from concentrate in contact with awaruite containing small blebs of pentlandite and associated with a Ni-phosphide (C). Enlargement of the grain illustrated in Figure C. X-ray elemental distribution map for Ni (E), Co (F), Fe (G), P (H), S (I). Scale bar in Figure D is 10 μm .

Gerakini-Ormylia (Greece) ophiolites, characterized by the formula $(\text{Ni,Fe})_5\text{P}$ (Zaccarini et al., 2016; Sideridis et al., 2018).

The Othrys Mo-phosphide is white-yellowish in color and isotropic (Figures 3F, 4 B,D,F). The mineral shows higher reflectance values than those of the other phosphides analyzed in the present work (Figure 5C, Table 2).

V-sulfide, ideally VS

Three small grains of a V-sulfide, less than 20 microns in size, have been found associated with awaruite, melliniite, and V-Ni phosphides (Figures 4 C,D,E,F,G,H). They all have almost identical composition (Table 1) corresponding to the empirical formula $(\text{V}_{0.95}\text{Fe}_{0.01}\text{Co}_{0.01}\text{Ni}_{0.02}\text{Mo}_{0.1})_{\Sigma 1}\text{S}$. This mineral was never found before in the Othrys chromitite, and it may actually represent a new vanadium species. Its composition does not fit those reported for the only natural V-sulfide accepted by IMA so far (e.g. patronite, VS_4 ; Hewett, 1910). The mineral is grey-pinkish in colour (Figures 4 D,F,H) similar to pyrrhotite, but is isotropic

in reflected light microscopy. The pinkish colour and the stoichiometry point to the divalent valence state for V. This is not surprising given the strong reducing conditions needed to form the mineralogical assemblage described in this paper.

The measured reflectivity is considerably lower than that of the associated phosphides (Figure 5D, Table 2). Based on the chemical composition and the optical properties, VS could be the equivalent of the cubic sulfides sphalerite $(\text{Zn,Fe})\text{S}$, rudashevskyite $(\text{Fe,Zn})\text{S}$, hawleyite CdS and metacinnabar HgS .

DISCUSSION AND CONCLUSIONS

The investigation of heavy accessory minerals from chromitites is challenging due to the typically small size of the recovered grains, their scarcity, and random distribution. Common methodologies rely on in situ techniques based on scanning of polished-thin sections by optical and electron microscopes that involve exploration of a small portion of sample. However, the study of concentrates provides a greater bulk and more extensive range of heavy minerals. Therefore, the study of the

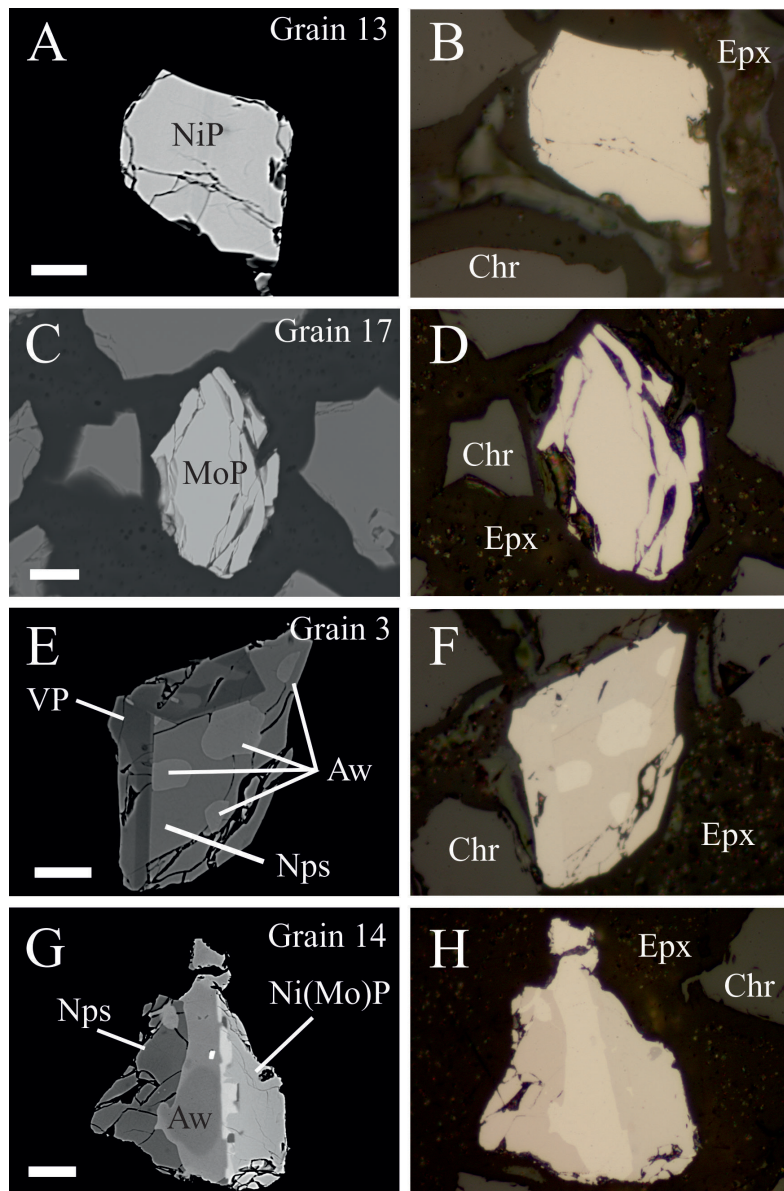


Figure 3. BSE images (A, C, E, G) and digital image in reflected plane polarized light (B, D, F, H) showing the potential new minerals and their association from the chromitite of Agios Stefanos. Abbreviations: NiP = Ni-allabogdanite or Ni-barringerite, Epx = epoxy, Chr = chromite, MoP = Mo-phosphide, VP = V-allabogdanite or V-barringerite, Aw = awaruite, Nps = nickelposphide, Ni(Mo)P = Ni-phosphide enriched in Mo.

concentrates can provide a better characterization of the heavy-mineral assemblage and composition and allows to improve the statistical basis for mineralogical and petrologic conclusions that can be drawn (Rudashevsky et al., 2002). However, the study of minerals concentrates involves some disadvantages, among which is the loss of in situ textural information and possible introduction of undesired contaminant minerals into the sample. These can include base metals alloys, diamonds, corundum and carbides, compounds that are widely used in sample

preparation. Therefore, this has generated a justified skepticism in the scientific community concerning the true (natural vs. artifact) provenance of such exotic minerals.

Being aware of these problems, and to avoid any possible controversy, all the steps of the sample collection and preparation were carefully checked. Field sampling in the Agios Stefanos mine was performed using a common steel hammer. The sample was ground using a laboratory apparatus manufactured by TM-Engineering with media Alloy 1 composed of Cr and Mo. This material is very

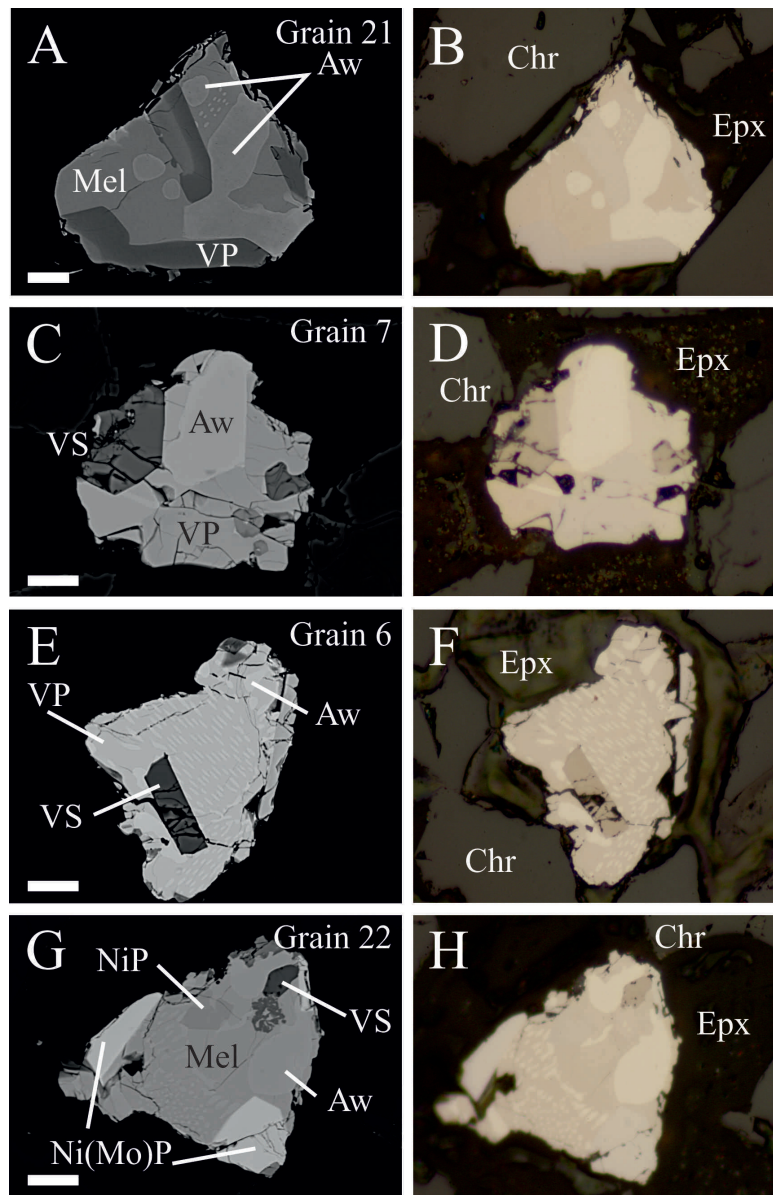


Figure 4. BSE images (A, C, E, G) and digital image in reflected plane polarized light (B, D, F, H) showing the potential new minerals and their association form the chromitite of Agios Stefanos. Abbreviations: Mel = melliniite, VS = vanadium mono-sulfide, others as in Figure 2.

hard and is recognized to be the best for applications where abrasion and impact is the norm. Furthermore, we ascertain that grinder does not consist of a Ni-Fe superalloy with phosphide brazing filler. The minerals analyzed in this work consist of a great variety of metals (Fe, Ni, Co, V, Mo) combined with P and S. Although these metals may occur individually as trace components of common steel, it is very difficult to explain how they could concentrate and combine with P and S to form such complex compounds during sample collection and preparation, and, even more important, how they could

become part of the mineralogical assemblage showing intergrowths with rock-forming minerals. Indeed, the minerals occur closely associated, or even inter-grown, with natural phases, e.g., chromite, chlorite, quartz, silicate-glass, awaruite, pentlandite, melliniite, nickelporphide, tiemannite (Ifandi et al., 2018 and present work) that is a strong indication of their natural origin. This assumption is also supported by the fact that many other chromitites treated with the same technique in the same laboratory, were not found to contain a phosphide-sulfide assemblage comparable with the one reported from the Agios Stefanos

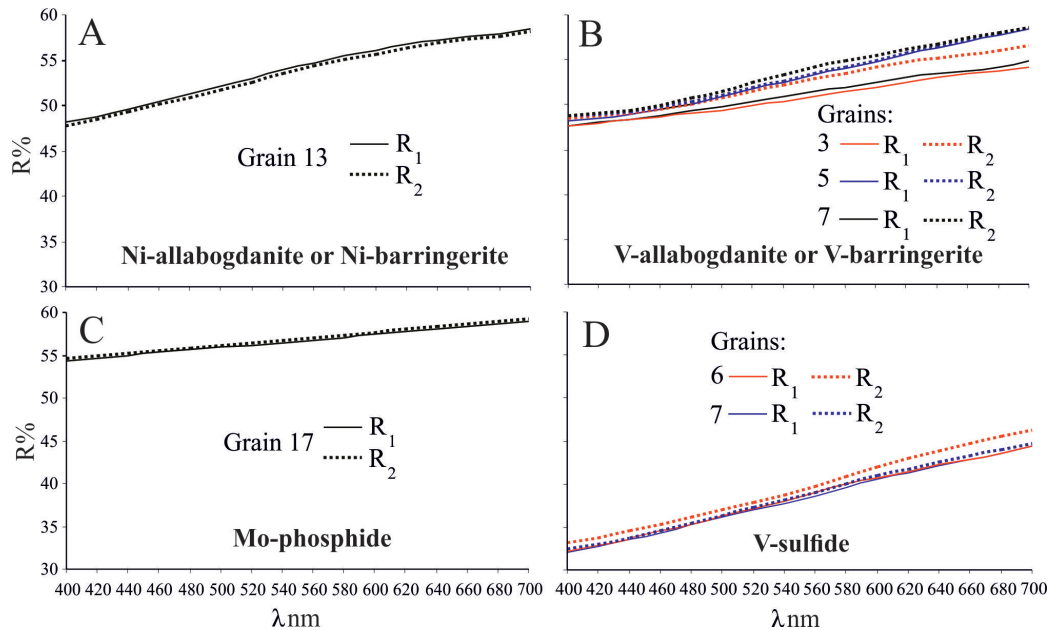


Figure 5. Reflectance data for selected potential new minerals from the Othrys chromitite. The reflectance values ($R\%$) are plotted versus the wavelength λ in nm.

sample (Kapsiotis et al., 2010; Grammatikopoulos et al., 2011; Tsikouras et al., 2016).

Although we can safely accept that the minerals described herein are not artifacts, their origin, provenance and interpretation is not straightforward. Metal sulfides and phosphides in ultramafic rocks are common indicators of low fO_2 and local reducing conditions of crystallization.

Magmatic precipitation of chromitite in the ophiolitic upper mantle is commonly attributed to the interaction of a residual peridotite (mainly harzburgite) with upwards flowing basaltic melts (MORB to boninites) at spreading centers or supra-subduction zones (Irvine, 1967; Dick and Bullen, 1984; Arai, 1997). The oxygen fugacity calculated from the chromite-olivine equilibrium usually fluctuates around the FMQ buffer (Ballhaus, et al., 1991; Chashchukhin et al., 1998; Garuti et al., 2012) that would be probably very high for primary precipitation of ultra-reduced accessory phases. Xiong et al. (2017) suggested that ultra-reducing conditions during formation of chromitite in the upper mantle can be locally achieved if the peridotite-melt interaction occurs in the presence of mantle-derived fluids enriched in CH_4 and H_2 . To support this conclusion Xiong et al. (2017) reported the presence of carbides, nitrides, silicides and other native metals (but not phosphides). The composition of chromite from the sample locality in the Agios Stefanos mine, is lower than expected for boninite-derived spinel and displays relatively high concentrations of ferric iron ($Fe_2O_3=6.72-9.26$ wt%) compared to common ophiolitic chromitites,

not consistent with the required ultra-reducing conditions.

Alternatively, the reduced environment could have originated during serpentinization process in the upper mantle at low temperature. It is widely accepted that during the serpentinization of peridotites, reducing fluids containing dissolved H_2 are released from the reduction of H_2O (Berndt et al., 1996; Charlou, 2002; Seyfried et al., 2007; Klein et al., 2009; Marcaillou et al., 2011). Consequently, the alteration of peridotites may form a strongly reduced micro-environment (Malvoisin et al., 2012). These observations allowed Zaccarini et al. (2016), Ifandi et al. (2018) and Sideridis et al. (2018) to postulate that the phosphides and the associated minerals found in the ophiolitic chromitites of Othrys and Gerakini-Ormylia may have crystallized during the serpentinization process at low temperature. In a recent paper, Etiope et al. (2018) have demonstrated that, among several ophiolitic rocks in Greece, i.e., serpentinite, peridotite, chromitite, gabbro, rodingite and basalt, only chromitites, including those of the complex Othrys, host considerable amounts of abiotic methane. Moreover, Agios Stefanos chromitite, is considered as the source rock of abiotic CH_4 measured in the west Othrys springs (Etiope et al., 2013; Etiope et al., 2018). The chromitite body is penetrated by rodingitized gabbro dykes and the alteration pattern of the interstitial peridotite, adjacent to rodingites, includes clinocllore+Cr-hydrogrossular+millerite+Mo-Co-Ni-V phosphides+magnetite and matches well the simulated serpentinization of harzburgite at 25 °C (Palandri and

Reed, 2004). Furthermore, these simulations show that a gas phase consisted of H_2 , H_2O and CH_4 is formed under generally dry conditions ($\log \text{ water/rock} < 1.5$), which is highly compatible with the formation of CH_4 in the studied chromitites. This further agrees with Etiope et al. (2018), who suggested that the CH_4 formation occurred at temperatures below $150^\circ C$ via Sabatier reaction, during the serpentinization process, providing further evidence that reducing condition can be achieved at low temperature during the alteration of mantle derived rocks. The phosphide assemblage of Agios Stefanos is systematically associated with Co-rich awaruite that, in turn, appears as a secondary product of the reduction (i.e. desulfidation) of pentlandite. Reduction of primary magmatic sulfides with formation of Fe-Ni alloys (mainly awaruite) typically accompanies the serpentinization of peridotites at low temperature (Eckstrand, 1975). This is in good agreement with the simulations from Palandri and Reed (2004), which show that under low temperature serpentinization and highly reducing environment, desulfurization occurs and the prevailing sulfide is gradually replaced by a phase with higher metal to sulfide ratio, as the water/rock ratio decreases (e.g., pyrite to pyrrhotite, pyrite+millerite to heazlewoodite, here Copentlandite to Co-awaruite).

Alternatively, as proposed by Britvin et al. (2015), the origin of the phosphide mineralization of the pyrometamorphic rocks related to the Hatrurim Formation, also known as a “Mottled Zone”, where nickolayite was discovered (Murashko et al., 2019), could be linked to coal-based reduction of phosphates, as it is widely employed in the industrial production of ferrophosphorus. The combustion of either bituminous rocks or methane originated from mud volcanoes could provide the environment sufficient for the direct reduction of natural phosphates and trevorite into Fe-Ni phosphides.

Based on laboratory experiments (Ballhaus et al., 2017) and the documented presence of phosphides in fulgurites (Pasek et al., 2013), Ifandi et al. (2018) did not discard the possibility that the ultra-reduced minerals of the Agios Stefanos may have formed during the interaction of their host rock with a surface lightning strike. The fulgurite-hypothesis gives way to the more fantastic model involving the impact of a meteorite on the mineralized ultramafic rocks. But we feel to immediately discard it because of the absence of high-pressure minerals in our assemblage, which had to be formed during the impact.

Most of the natural phosphides have been discovered in meteorites (Britvin et al., 1999, 2002; Zolensky et al., 2008; Buseck, 1969; Ivanov et al., 2000; Pratesi et al., 2006; Ma et al., 2014; Skala and Cisarova, 2005), formed in a vastly different environment comparing with the assemblage reported in this study. However, we believe

that ultra-reducing conditions is the common factor that links the extraterrestrial phosphides reported in the literature with the phosphides described here in.

In conclusion, the genetic interpretation of the minerals newly discovered in the Othrys ophiolite still remains speculative and open to further discussion, due to the lack of experimental work on the stability conditions of phosphides and sulfides with the composition reported in this contribution. However, we can conclude that, based on the chemical data, some of the discovered minerals potentially represent new mineral species. The finding of homogenous grains up to $80\ \mu m$ in size, encourages us to provide the crystallographic investigation required for the acceptance as new mineral by the IMA Commission. The finding of homogenous grains up to $80\ \mu m$ in size, encouraged us to provide the crystallographic investigation required for the acceptance as new mineral by the IMA Commission. Preliminary data are available and the entire procedure for the final acceptance will be completed soon.

ACKNOWLEDGMENTS

The authors are grateful to the University Centrum for Applied Geosciences (UCAG) for the access to the E. F. Stumpfl electron microprobe laboratory. SGS Mineral Services, Canada, is thanked to have performed the concentrate sample. We are grateful to Paolo Ballirano for his editorial handling. Two anonymous referees are thanked for their support. Sofia Karipi is thanked for sample collection and participating in the field work.

REFERENCES

- Arai S., 1997. Control of Wall-rock Composition on the Formation of Podiform Chromitites as a Result of Magma-Peridotite Interaction. *Resource Geology* 47, 177-187.
- Ballhaus C., Berry R.F., Green, D.H., 1991. High-pressure experimental calibration of the olivine-orthopyroxene-spinel geobarometer: Implications for the oxidation state of the upper mantle. *Contribution to Mineralogy and Petrology* 107, 27-40.
- Ballhaus C., Wirth R., Fonseca R.O.C., Blanchard H., Pröll W., Bragagni A., Nagel T., Schreiber A., Dittrich S., Thome V., Hezel D.C., Below R., Cieszynski H., 2017. Ultra-high pressure and ultra-reduced minerals in ophiolites may form by lightning strikes. *Geochemical Perspectives Letters* 5, 42-46.
- Berndt M.E., Allen D.E., Seyfried W.E., 1996. Reduction of CO_2 during serpentinization of olivine at $300^\circ C$ and 500 bar. *Geology* 24, 351-354.
- Britvin S.N., Kolomensky V.D., Boldyreva M.M., Bogdanova A.N., Krester Y.L., Boldyreva O.N., Rudashevsky N.S., 1999. Nickelphosphide $(Ni,Fe)_3P$ -The nickel analogue of schreibersite. *Zapiski Vserossiiskogo mineralogicheskogo obshchestva* 128, 64-72.
- Britvin S.N., Rudashevskii N.S., Krivovichev S.V., Burns

- P.C., Polekhovsky Y.S., 2002. Allabogdanite, (Fe,Ni)₂P, a new mineral from the Onello meteorite: The occurrence and crystal structure. *American Mineralogist* 87, 1245-1249.
- Britvin S.N., Vapnik Y., Polekhovsky Y.S., Krivovichev S.V., 2013. CNMNC Newsletter No. 15, February 2013. *Mineralogical Magazine* 77, 1-12.
- Britvin S.N., Murashko M.N., Vapnik Y., Polekhovsky Y.S., Krivovichev S.V., 2014. CNMNC Newsletter No. 19, February 2014. *Mineralogical Magazine* 78, 165-170.
- Britvin S.N., Murashko M.N., Vapnik Y., Polekhovsky Y.S., Krivovichev S.V., 2015. Earth's Phosphides in Levant and insights into the source of Archean prebiotic phosphorus. *Scientific Reports* 5, 8355.
- Britvin, S.N., Murashko, M.N., Vapnik, Y., Polekhovsky, Y.S., Krivovichev, S.V., Vereshchagin, O.S., Vlasenko, N.S., Shilovskikh, V.V., Zaitsev, A.N., 2018. Zuktamrurite, FeP₂, a new mineral, the phosphide analogue of löllingite, FeAs₂. *Physics and Chemistry of Minerals*. doi: org/10.1007/s00269-018-1008-4.
- Britvin, S.N., Vapnik, Y., Polekhovsky, Y.S., Krivovichev, S.V., Krzhizhanovskaya, M.G., Gorelova, L.A. Vereshchagin, O.S., Shilovskikh, V.V., Zaitsev, A.N. 2019. Murashkoite, FeP, a new terrestrial phosphide from pyrometamorphic rocks of the Hatrurim Formation, South Levant. *Mineralogy and Petrology* 113, 237-248.
- Buseck P.R., 1969. Phosphide from meteorites: Barringerite, a new iron-nickel mineral. *Science* 165, 169-171.
- Chashchukhin I.S., Votyakov S.L., Uimin S.G., 1998. Oxygen thermometry and barometry in chromite-bearing ultramafic rocks: An example of ultramafic massifs on the Urals. II. Oxidation state of ultramafics and the composition of mineralizing fluids. *Geochemistry International* 36, 783-791.
- Charlou J., 2002. Geochemistry of high H₂ and CH₄ vent fluids issuing from ultramafic rocks at the Rainbow hydrothermal field (36°14'N, MAR). *Chemical Geology* 191, 345-35.
- Dick H.J.B. and Bullen T., 1984. Chromian spinel as a petrogenetic indicator in abyssal and alpine-type peridotites and spatially associated lavas. *Contribution to Mineralogy and Petrology* 86, 54-76.
- Economou M., Dimou E., Economou G., Migiros G., Vacondios I., Grivas E., Rassios A., Dabitzias S., 1986. In: W. Petrascheck, S. Karamata, G.G. Kravchenko, Z. Johan, M. Economou, T. Engin, (Eds.), *Chromites, UNESCO's IGCP197 project metallogeny of ophiolites*. Theophrastus Publ. S.A., Athens, 129-159.
- Eckstrand O.R., 1975: The Dumont serpentinite: A model for control of Nickeliferous opaque mineral assemblages by alteration reactions in ultramafic rocks. *Economic Geology* 70, 183-201.
- Etiopé G., Ifandi E., Nazzari M., Procesi M., Tsikouras B., Ventura G., Steele A., Tardini R., Sztamari P., 2018. Widespread abiotic methane in chromitites. *Scientific Reports* 8, 8728.
- Etiopé G., Tsikouras B., Kordella S., Ifandi E., Christodoulou D., Papatheodorou G., 2013. Methane flux and origin in the Othrys ophiolite hyperalkaline springs, Greece. *Chemical Geology* 347, 161-174.
- Garuti G., Pushkarev E., Thalhammer O.A.R., Zaccarini F., 2012. Chromitites of the Urals (Part 1): Overview of chromite mineral chemistry and geo-tectonic setting. *Ophioliti* 37, 27-53.
- Garuti G., Zaccarini F., Economou-Eliopoulos M., 1999. Paragenesis and composition of laurite from chromitites of Othrys (Greece): Implications for Os-Ru fractionation in ophiolite upper mantle of the Balkan Peninsula. *Mineralium Deposita* 34, 312-319.
- Grammatikopoulos T.A., Kapsiotis A., Tsikouras B., Hatzipanagiotou K., Zaccarini F., Garuti G., 2011. Spinel composition, PGE geochemistry and mineralogy of the chromitites from the Vourinos ophiolite complex, northwestern Greece. *Canadian Mineralogist* 49, 1571-1598.
- Hewett, D.F., 1910. Vanadium Deposits in Peru. *Transactions of the American Institute of Mining, Metallurgical Engineering* 40, 274-29.
- Ifandi E., Zaccarini F., Tsikouras B., Grammatikopoulos T., Garuti G., Karipi S., Hatzipanagiotou K., 2018. First occurrences of Ni-V-Co phosphides in chromitite of Agios Stefanos mine, Othrys ophiolite, Greece. *Ophioliti* 43, 131-145.
- Irvine T.N., 1967. Chromian spinel as a petrogenetic indicator. Part II. Petrological Application. *Canadian Journal of Earth Sciences* 4, 71-103.
- Ivanov A.V., Zolensky M.E., Saito A., Ohsumi K., Yang S.V., Kononkova N.N., Mikouchi T., 2000. Florenskyite, FeTiP, a new phosphide from the Kaidun meteorite. *American Mineralogist* 85, 1082-1086.
- Jaszczak J.A., Rumsey M.S., Bindi L., Hackney S.A., Wise M.A., Stanley C.J., Spratt J., 2016. Merelaniite, Mo₄Pb₄V₅Sb₁₅, a New Molybdenum-Essential Member of the Cyndrite Group, from the Merelani Tanzanite Deposit, Lelatema Mountains, Manyara Region, Tanzania. *Minerals* 6. doi: org/10.3390/min6040115.
- Kapsiotis A., Grammatikopoulos T.A., Tsikouras B., Hatzipanagiotou K., 2010. Platinum-group mineral characterization in concentrates from high-grade PGE Al-rich chromitites of Korydallos area in the Pindos ophiolite complex (NW Greece). *Resource Geology* 60, 178-191.
- Klein F., Bach W., Jöns N., McCollom T., Moskowicz B., Berquo T., 2009. Iron partitioning and hydrogen generation during serpentinization of abyssal peridotites from 15°N on the Mid Atlantic Ridge. *Geochimica et Cosmochimica Acta* 73, 6868-6893.
- Kovalenker V.A., Evstigneeva T.L., Malov V.S., Trubkin N.V., Gorshkov A.I., Geinke V.R., 1984. Nekrasovite Cu₂₆V₂Sn₆S₃₂ - a new mineral of the colusite group. *Mineralogiceskij Zhurnal* 6, 88-97.
- Ma C., Beckett J.R., Rossman G.R., 2014. Monipite, MoNiP, a new phosphide mineral in a Ca-Al-rich inclusion from the

- Allende meteorite. *American Mineralogist* 99, 198-205.
- Malvoisin B., Chopin C., Brunet F., Matthieu, E., Galvez M.E., 2012. Low-temperature Wollastonite formed by carbonate reduction: a marker of serpentinite redox conditions. *Journal of Petrology* 53, 159-176.
- Marcaillou C., Muñoz M., Vidal O., Parra T., Harfouche M., 2011. Mineralogical evidence for H₂ degassing during serpentinization at 300 °C/300 bar. *Earth Planetary Science Letters*, 303: 281-290.
- Murashko M.N., Vapnik Y., Polekhovskiy Y.P., Shilovskikh V.V., Zaitsev A.M., Vereshchagin O.S., Britvin S.N., 2019. Nickolayite, IMA 2018-126. CNMNC Newsletter No. 47, February 2019. *European Journal of Mineralogy* 31, 199-204.
- Oryshchyn S.V., Le Sénéchal C., Députier S., Bauer J., Guerin R., Akselrud L.G., 2001. New Ternary Phases in the Mo-Ni-P System: Synthesis and Crystal Structures. *Journal of Solid State Chemistry* 160, 156-166.
- Ostrooumov M., Taran Y., Arellano-Jimenez M., Ponce A., Reyes-Gasca J., 2009. Colimaite, K₃VS₄ - a new potassium-vanadium sulfide mineral from the Colima volcano, State of Colima (Mexico). *Revista Mexicana de Ciencias Geológicas* 26, 600-608.
- Palandri J.L. and Reed M.H., 2004. Geochemical models of metasomatism in ultramafic systems: Serpentinization, rodingitization, and sea floor carbonate chimney precipitation. *Geochimica et Cosmochimica Acta* 68, 1115-1133.
- Pasek M.A., Hammeijer J.P., Buick R., Gull M., Atlas Z., 2013. Evidence for reactive reduced phosphorus species in the early Archean ocean. *Proceeding Natural Academy of Sciences* 110, 100089-100094.
- Pratesi G., Bindi L., Moggi-Cecchi V., 2006. Icosahedral coordination of phosphorus in the crystal structure of melliniite, a new phosphide mineral from the Northwest Africa 1054 acapulcoite. *American Mineralogist* 91, 451-454.
- Rassios A. and Smith A.G., 2001. Constraints on the formation and emplacement age of western Greek ophiolites (Vourinos, Pindos, and Othris) inferred from deformation structures in peridotites. In: Dilek Y., Moores E., Elthon D. and Nicolas, A. (Eds.), *Ophiolites and Oceanic Crust: New Insights from Field Studies and the Ocean Drilling Program*. Geol. Soc. Am. Spec. Pap., Boulder, Colorado, 473-484.
- Rudashevsky N.S., Garuti G., Andersen J.C.Ø, Kretser Yu. L., Rudashevsky V.N., Zaccarini F., 2002. Separation of accessory minerals from rocks and ores by hydroseparation (HS) technology: Method and application to CHR-2 chromitite, Niquelândia intrusion, Brazil. *Transactions of the Institutions of Mining and Metallurgy, Section B: Applied Earth Science* 111, B87-B94.
- Seyfried W.E., Foustoukos D.I., Fu Q., 2007. Redox evolution and mass transfer during serpentinization: An experimental and theoretical study at 200 °C, 500 bar with implications for ultramafic-hosted hydrothermal systems at mid-ocean ridges. *Geochimica et Cosmochimica Acta* 71, 3872-3886.
- Sideridis A., Zaccarini F., Grammatikopoulos T., Tsitsanis P., Tsikouras B., Pushkarev E., Garuti G., Hatzipanagiotou K., 2018. First occurrences of Ni-phosphides in chromitites from the ophiolite complexes of Alapaevsk, Russia and GerakiniOrmylia, Greece. *Ofioliti* 43, 75-84.
- Skala R. and Cisarova I., 2005. Crystal structure of meteoritic schreibersites: determination of absolute structure. *Physics and Chemistry of Minerals* 31, 721-732.
- Spiridonov E.M., Kachalovskaya V.M., Kovachev V.V., Krapiva L.Y., (1992a). Germanocolusite Cu₂₆V₂(GeAs)₆S₃₂ - a new mineral. *Vestnik Moskovskogo Universiteta, Geologiya* 6, 50-54 (in Russian).
- Spiridonov E.M., Badalov A.S., Kovachev V.V., 1992b. Stibiocolusite Cu₂₆V₂(Sb,Sn,As)₆S₃₂: A new mineral. *Doklady Akademii Nauk* 324, 411-414 (in Russian).
- Trojer F.J., 1966. Refinement of the structure of sulvanite. *American Mineralogist* 51, 890-894.
- Tsikouras B., Ifandi E., Karipi S., Grammatikopoulos T.A., Hatzipanagiotou K., 2016. Investigation of Platinum-Group Minerals (PGM) from Othrys Chromitites (Greece) using superpanning concentrates. *Minerals* 6. doi: 10.3390/min6030094.
- Xiong Q., Griffin W.L., Huang J.X., Gain S.E.M., Toledo V., Pearson N.J., O'Reilly S.Y., 2017. Super-reduced mineral assemblages in "ophiolitic" chromitites and peridotites: the view from Mount Carmel. *European Journal of Mineralogy* 29, 557-570.
- Zaccarini F., Pushkarev E., Garuti G. and Kazakov I., 2016. Platinum-Group Minerals and other accessory phases in chromite deposits of the Alapaevsk ophiolite, Central Urals, Russia. *Minerals* 6. doi: 10.3390/min6040108.
- Zachariasen W.H., 1933. X-Ray examination of colusite, (Cu,Fe,Mo,Sn)₄(S,As,Te)₃₋₄. *American Mineralogist* 18, 534-537.
- Zolensky M., Gounelle M., Mikouchi T., Ohsumi K., Le L., Hagiya K., Tachikawa O., 2008. Andreyivanovite: A second new phosphide from the Kaidun meteorite. *American Mineralogist* 93, 1295-1299.



This work is licensed under a Creative Commons Attribution 4.0 International License CC BY. To view a copy of this license, visit <http://creativecommons.org/licenses/by/4.0/>

